

# Thermally Stable and Solvent-Resistant Conductive Polymer Composites with Cross-Linked Siloxane Network

Zhifan Ke, Liyan You, Dung T. Tran, Jiazhi He, Kuluni Perera, Aristide Gumyusenge, and Jianguo Mei\*

Cite This: *ACS Appl. Polym. Mater.* 2021, 3, 1537–1543

Read Online

ACCESS |



Metrics &amp; More



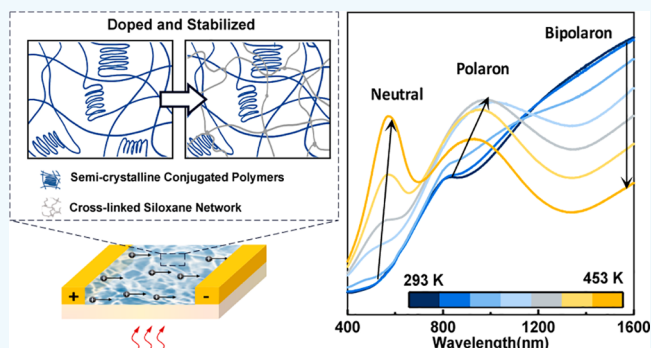
Article Recommendations



Supporting Information

**ABSTRACT:** Doped conjugated polymers can present high electrical conductivity, but their stability against external stimuli such as heat, moisture, and solvent is often limited. Here, we report a design approach to render thermally and chemically stable conductive polymer composites consisting of 3,4-propylenedioxythiophene (ProDOT) and ethylenedioxythiophene (EDOT) based copolymers (CPs) and cross-linkable chlorosilane (C-Si). Through a sol–gel reaction, chlorosilane precursors form siloxane networks and simultaneously dope the polymers. Temperature-dependent *in situ* UV–vis absorption and conductivity characterization show that the conductive C-Si/CPs composites can retain their doped state at high temperature and in prolonged baking time. Specifically, the composites' conductivity remains almost unchanged after 6 h and only slightly dipping to nearly 80% after 24 h of annealing at 80 °C in ambient air. They also exhibit excellent solvent resistance upon dipping into water and chloroform. This work reports a method of designing stable-doped polymer systems that can function under harsh conditions.

**KEYWORDS:** doped conjugated polymers, thermal stability, cross-linkable chlorosilane, cross-linked siloxane network, solvent-resistant



## 1. INTRODUCTION

Doping is a powerful means to improve the electrical conductivity of conjugated polymers,<sup>1,2</sup> which is widely practiced in thermoelectrics (OTEs)<sup>3–6</sup> and transparent electrodes.<sup>3,7,8</sup> However, organic doping is typically unstable under high temperature. For instance, thermal stress often induces conformational changes of polymer chains, and results in morphological disorder in conjugated polymer thin films.<sup>9</sup> In doped thin films, this process is often accompanied by the expelling of dopant molecules, causing a decrease of conductivity and degradation of device performance.<sup>10,11</sup> Molecular dopants such as ferric chloride<sup>12,13</sup> or 2,3,5,6-tetrafluoro-7,7,8,8-tetracyanoquinodimethane (F4-TCNQ)<sup>14,15</sup> enable effective doping of conjugated polymers, whereas they tend to diffuse at high temperature because of their relatively small sizes.<sup>16,17</sup> To improve thermal stability, large-sized dopants have been used but usually required sophisticated syntheses. Also, oversized dopants could heavily degrade polymer packing and reduce device performance.<sup>16,18</sup> Therefore, a new approach to improve the thermal stability of doped conjugated polymer is still needed.

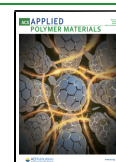
We hypothesize that framing a conjugated polymer into a cross-linked network could stabilize polymer morphology and thus benefit doping stability.<sup>19</sup> We previously showed that blending semicrystalline conjugated polymers with high glass-transition temperature ( $T_g$ ), insulating polymers at a controlled

ratio, enabled the formation of a thermally stable thin film. Highly stable charge transport behaviors have been observed for the blended thin films at the temperature as high as 220 °C in transistors.<sup>20,21</sup> Besides, a cross-linked network has been proven to stabilize the morphology of conductive polymer film but there are no reports explicitly using this approach for improving thermal stability to date. Wang et al. reported that adding cross-linked polystyrene could improve the environmental stability of FeCl<sub>3</sub>-doped poly(3-octylthiophene) (P3OT) by minimizing the movement of doped polymer chains.<sup>12</sup> Furthermore, silane cross-linkers, for example, glycidoxy propyltrimethoxysilane (GOPS), are often added to poly(3,4-ethylenedioxythiophene) polystyrenesulfonate (PEDOT:PSS) to prevent film delamination and stabilize film morphology in aqueous environments through the formation of siloxane networks.<sup>22–24</sup> However, the formed cross-linked networks often lower the conductivity of the thin films because of their insulating nature. Currently, the insight

Received: December 15, 2020

Accepted: February 1, 2021

Published: February 8, 2021



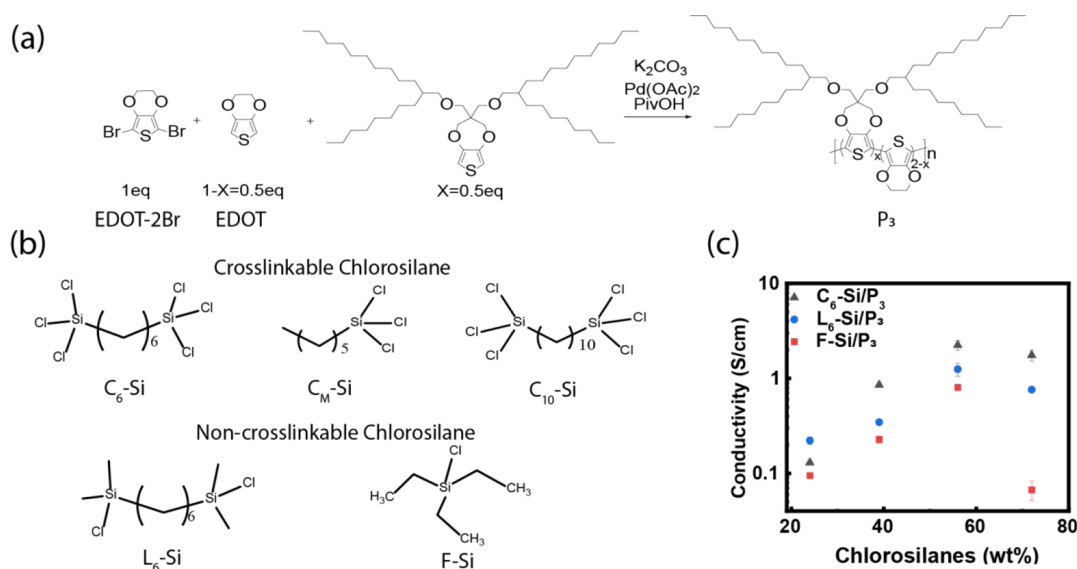


**Figure 1.** (a) Synthetic route for Prododt-EDOT copolymers  $P_1$ – $P_3$ , in which  $X = 1, 0.67,$  and  $0.5$  are for  $P_1, P_2$  and  $P_3$ , respectively; (b) chemical structures of different chlorosilanes; (c) conductivities of three chlorosilanes/ $P_3$  composites with varying percentages of chlorosilanes in the mixed solutions.

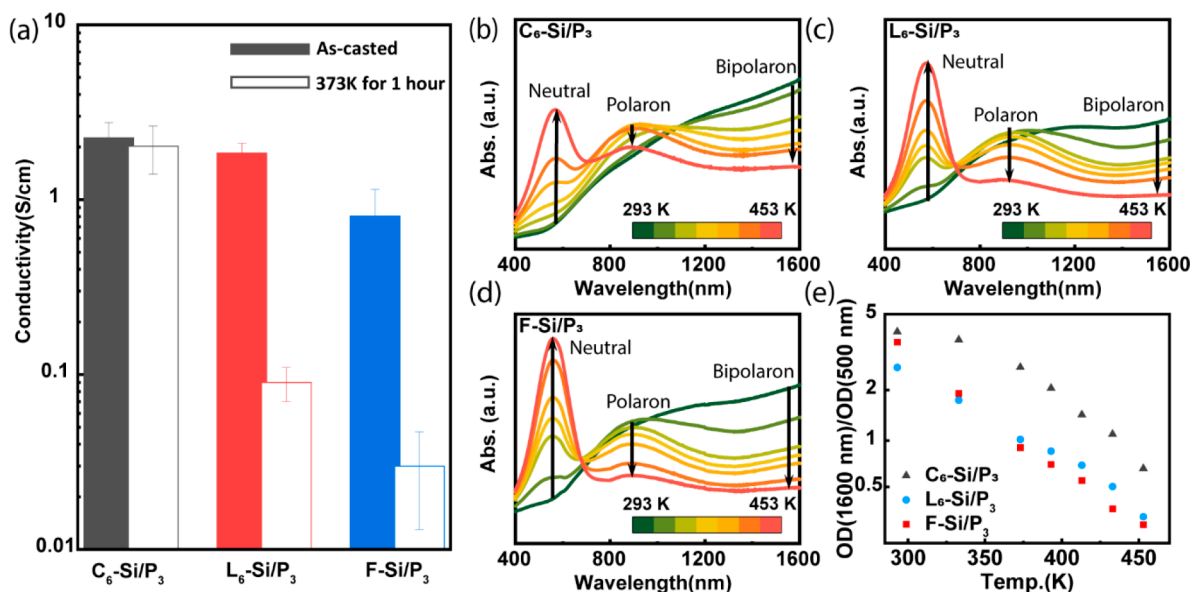


**Figure 2.** Thermal stability of different chlorosilanes/ $P_3$  composite. (a) Conductivity comparison of different composites before and after annealing at 373 K for 1 h with the solid color bars indicating the as-casted performance and the transparent bars indicating the performance after annealing; *In situ* temperature-dependent UV–vis absorption of (b)  $C_6$ -Si/ $P_3$ , (c)  $L_6$ -Si/ $P_3$ , and (d)  $F$ -Si/ $P_3$  when increasing temperature from 293 to 453 K; (e) optical density ratio between 1600 and 500 nm for different chlorosilanes/ $P_3$  composites at elevating temperature.

into the role of cross-linked networks in the thermal stability of conductive polymers is lacking.

To confirm the hypothesis that cross-linked networks could improve the thermal stability of the doped composites, the stabilities of different chlorosilane-doped CPs were evaluated. First, we selected three chlorosilanes precursors, namely 1,6-bis(trichlorosilyl)hexane (cross-linkable silane;  $C_6$ -Si), 1,6-bis(chlorodimethylsilyl)hexane (linear silane;  $L_6$ -Si) and chlorotriethylsilane (flowable silane;  $F$ -Si) and mixed them with conjugated polymer  $P_3$ . Cross-linkable chlorosilanes ( $C$ -Si) can readily form siloxane networks and have been used extensively as precursors for cross-linked inorganic/organic hybrid materials.<sup>25–27</sup> Besides, previous research demonstrated several conjugated polymers can be doped by alkyl silanes,

resulting in enhanced conductivity and improved transistor performance.<sup>26,28</sup> As expected, although all of the chlorosilanes can dope  $P_3$ , only  $C_6$ -Si can form a cross-linked matrix and thus its composite demonstrates superior thermal stability compared to those of its counterparts. Next, we tested the influence of the rigidity of the matrix on the composite thermal stability by tuning the structure of the  $C$ -Si. Here, the monosubstituted trichlorosilane ( $C_M$ -Si), which forms the most rigid network, shows the best temperature robustness. When being baked at 373 K under ambient conditions, the conductivity of the composites barely changed after 6 h and maintained nearly 80% of the initial conductivity after 24 h. The solvent resistance of  $C$ -Si/CPs is also confirmed by dipping the films into water and chloroform. Finally, after

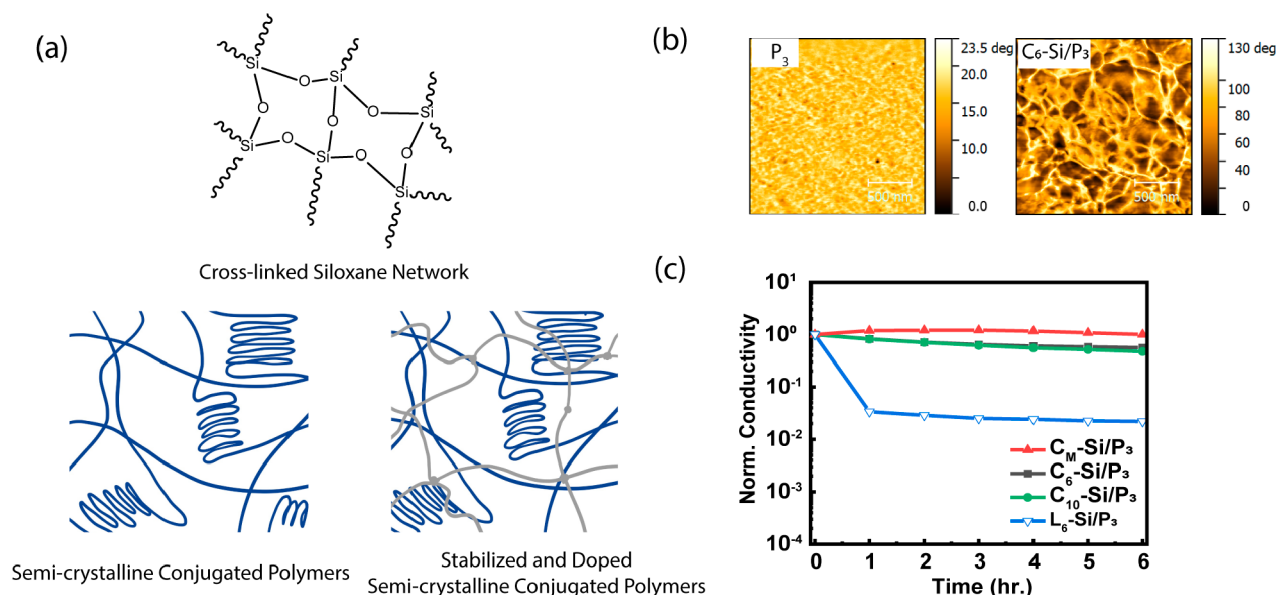


**Figure 3.** (a) Chemical structures of cross-linked siloxane network and proposed schematic description of C-Si/P<sub>3</sub> composites; (b) AFM phase images of pure P<sub>3</sub> and C<sub>6</sub>-Si/P<sub>3</sub> at 56 wt % of C<sub>6</sub>-Si; (c) normalized conductivities of chlorosilane/P<sub>3</sub> composites (normalized at time = 0 h) with different 56 wt % chlorosilane precursors when baked at 353 K under ambient conditions for 6 h.

finding the most stable dopant, we tested the compatibility of C<sub>M</sub>-Si with different Prodot-EDOT copolymers (P<sub>1</sub>, P<sub>2</sub>, and P<sub>3</sub>). The low oxidation onset of these copolymers allows them to be readily doped and they have shown great potential as candidates of p-type thermoelectric and electrode material.<sup>3</sup> Among these three polymers, P<sub>3</sub> with the highest proportion of EDOT has the lowest oxidation level. As expected, P<sub>3</sub> has the best compatibility with the siloxane network and has the highest thermal stability among tested CPs.

## 2. RESULTS AND DISCUSSIONS

**2.1. The Thermal Stability of the Doped System with Cross-Linked Siloxane Network.** First, polymer P<sub>3</sub> is mixed with a cross-linkable chlorosilane (C<sub>6</sub>-Si) and two non-cross-linkable chlorosilanes (L<sub>6</sub>-Si, F-Si) (Figure 1a,b). All three additives, after forming the linked matrix, could dope the polymer, but the C<sub>6</sub>-Si outperforms the rest both in terms of conductivities as well as the thermal stability. Compared with pristine P<sub>3</sub> film, the conductivities of all the chlorosilanes/P<sub>3</sub> composites greatly increases, and the C<sub>6</sub>-Si/P<sub>3</sub> composite displays the greatest improvement, by six-orders of magnitude (Figure 1c, Figure S4) to 2 S/cm. The mechanism of chlorosilane-induced doping is reportedly associated with the generation of hydrogen chlorine and silanols during sol-gel reaction; the former one is a common p-type dopant and the latter one is well-known as electron traps.<sup>28–30</sup> With the increased content of chlorosilanes, the conductivities of all composites increase and reach the highest value when the weight percentage of the chlorosilanes in the mixed solution is 56% (Figure 1c). When the percentage of chlorosilanes goes above 60 wt %, composites' conductivities start to drop due to the formation of isolated conducting domains in the systems (Figure S5). The absorbance spectrum of all three composites also confirms that chlorosilanes dope the P<sub>3</sub> polymer, shown by the wide polaronic absorbance around 900–1000 nm, the bipolaronic absorbance around the 1600 nm, and the suppressed neutral peak at 550 nm (Figure S6).

The doped composite with a cross-linked siloxane network exhibits superior thermal stability compared to its counterparts. After annealing at 373 K for 1 h, C<sub>6</sub>-Si/P<sub>3</sub> maintains nearly 90% of their original electrical conductivity while the conductivities of L<sub>6</sub>-Si/P<sub>3</sub> and F-Si/P<sub>3</sub> drop over one order (Figure 2a). *In situ* temperature-dependent UV-vis absorption spectra of the three composites (Figure 2b–d) also confirm the superior doping stability of C<sub>6</sub>-Si/P<sub>3</sub> composites. As temperature increases, the bipolaron peak (~1600 nm) gradually drops and the neutral peak (~550 nm) increases in all three composites, indicating the dedoping process at high temperature. However, polaron peaks in L<sub>6</sub>-Si/P<sub>3</sub> and F-Si/P<sub>3</sub> composites monotonically decrease, indicating that the composites quickly dedope to neutral states. While the polaron peak of C<sub>6</sub>-Si/P<sub>3</sub> composites increases and then slightly falls only when temperature is above 413 K, indicating the transformation from bipolarons to polarons occurs from 293 to 393 K. Since the films' optical density (OD) of a different wavelength directly reflects the conductivities of the composites, the ratio between the bipolaronic signal (~1600 nm) and neutral signal (~550 nm) is used to indicate the conductivity change of the composites at elevated temperature. C<sub>6</sub>-Si has the highest optical density ratio (1600 nm/550 nm) at high temperature, indicating a large portion of C<sub>6</sub>-Si/P<sub>3</sub> is still doped even at 450 K (Figure 2e).

**2.2. Effect of Cross-Linked Siloxane Network on the Thermal Stability of Doped System.** The distinct difference between C<sub>6</sub>-Si/P<sub>3</sub> and the other two systems, L<sub>6</sub>-Si/P<sub>3</sub> and F-Si/P<sub>3</sub>, is attributed to the ability to form a cross-linked network by sol-gel reactions among the precursors. During film processing, C<sub>6</sub>-Si precursors cross-link with each other via the reaction at the terminal trichlorosilyl groups and form a cross-linked siloxane network in the composites; CPs are doped during the sol-gel reaction and expectedly confined by the network (Figure 3a).<sup>25</sup> The C<sub>6</sub>-Si/P<sub>3</sub> composites show phase separation (Figure 3b, Figure S7), and the formation of cross-linked network in the C<sub>6</sub>-Si/P<sub>3</sub> composites is further confirmed by the appearance of Si–O–Si stretching vibrations

at 1050 and 1150  $\text{cm}^{-1}$  in the Fourier transform infrared (FTIR) spectroscopic analysis (Figure S8a).<sup>31,32</sup> Besides, the Si–O–Si characteristic bands appear at room temperature and barely show any changes after thermal annealing, indicating the cross-linked siloxane network formation completes at room temperature (Figure S8b). On the contrary, without trichlorosilyl groups L<sub>6</sub>-Si and F-Si cannot form cross-linked siloxane networks. They formed different matrices during sol-gel reaction, which are named linear matrix and flowable matrix, respectively. L<sub>6</sub>-Si/P<sub>3</sub> and F-Si/P<sub>3</sub> composites maintain a similar smooth surface morphology as pure P<sub>3</sub> film (Figure S9) and show much lower Si–O–Si stretching vibrations bands in the FTIR spectra. On the basis of all of the observations, we proposed that the presence of the cross-linked siloxane network greatly enhances thermal stability of the composites as the cross-linked network effectively stabilizes film microscale morphology and prevents a dedoping process.

As a cross-linked network is demonstrated to improve the composite's stability, now we look for the best chlorosilanes available. We hypothesize that with a smaller number of spacer carbons, the network will be more rigid and thus could further improve the composites thermal stability.<sup>33,34</sup> Here, three cross-linkable chlorosilanes, hexyltrichlorosilane with monochlorosilyl (C<sub>M</sub>-Si) and 1,10-bis(trichlorosilyl)decane with 10 spacers (C<sub>10</sub>-Si) (Figure 1b), confirmed forming a cross-linked network (Figure S10, Figure S11), are compared with the previous used C<sub>6</sub>-Si and L<sub>6</sub>-Si/P<sub>3</sub> composites in a thermal stress test at 353 K in open air (Figure 3c). The C<sub>M</sub>-Si composite with the most rigid cross-linked network without flexible spacers in the cross-linkers shows the highest thermal stability. In the first hour, the electrical conductivity of the linear L<sub>6</sub>-Si/P<sub>3</sub> composites dropped over one order, as a result of lacking the cross-linked siloxane network. Conversely, all of the cross-linked C-Si/P<sub>3</sub> composites showed slightly increased conductivity, which is attributed to further condensation between active chlorosilane precursors induced by thermal stress. After 6 h, the C<sub>6</sub>-Si/P<sub>3</sub> and C<sub>10</sub>-Si/P<sub>3</sub> composites with flexible spacers in the siloxane network drop to about 60% of their as-spun conductivities, whereas C<sub>M</sub>-Si/P<sub>3</sub> composites could maintain their original conductivity (Figure 3c).

**2.3. Improved Solvent Resistance in the Cross-Linked Composites.** Besides improving thermal stability, the cross-linked siloxane network in C-Si/P<sub>3</sub> composites also significantly increases the composite solvent robustness. Reportedly, introducing cross-linked siloxane networks is commonly utilized to prepare ultrathin, chemically robust polymer dielectric layers<sup>30</sup> and pattern polymer semiconductors through photolithography.<sup>25</sup> First, the C<sub>M</sub>-Si/P<sub>3</sub> shows excellent water-resistance. After being immersed for 1 h, it maintains over 95% of its original conductivity (Figure 4a). The UV–vis absorption spectrum of C<sub>M</sub>-Si/P<sub>3</sub> composites overlaps with the original one after being dipped in water, and their in situ UV–vis absorption at 600 nm remains unchanged over 2000 s in water (Figure 4b, Figure S14). The superior water resistance of the polymer composites is due to the increased polymer chain entanglement.<sup>26</sup> Besides, the highly hydrophobic nature of cross-linked siloxane network can prevent the permeation of water molecules. Additionally, the C<sub>M</sub>-Si/P<sub>3</sub> composites exhibit greatly improved robustness to chloroform, which is the original solvent of chlorosilanes and CPs. On the one hand, the pure P<sub>3</sub> film is easily redissolved in CHCl<sub>3</sub>, shown by a clear color change (Figure S15b) and the greatly dropped absorption intensity after dipping in CHCl<sub>3</sub>

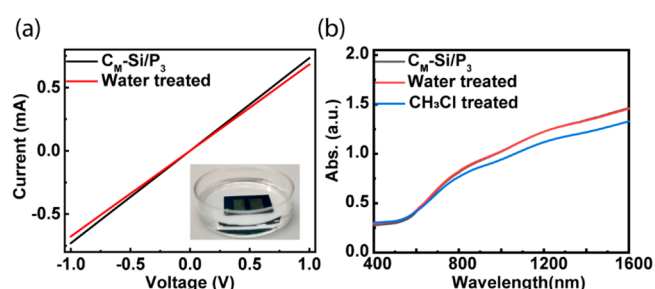


**Figure 4.** Solvent resistance of 56 wt % C<sub>M</sub>-Si/P<sub>3</sub> composites. (a) *I*–*V* curve for the samples before and after being immersed in water for 1 h; (b) UV–vis absorptions of 56 wt % C<sub>M</sub>-Si/P<sub>3</sub> composites before and after being dipped in water and CHCl<sub>3</sub>.

(Figure S15a). On the other hand, C<sub>M</sub>-Si/P<sub>3</sub> composite samples barely show any color change. Although the intensities of polaronic (~550 nm) and bipolaronic (~1600 nm) peaks slightly drop, the composite remains heavily doped (Figure 4b).

**2.4. Influence of Conjugated Polymers on the Thermal Stability of the Composite.** After finding the most robust cross-linker, we tested the effect of the compatibility of C<sub>M</sub>-Si with different Prodod-EDOT copolymers on the performance of the composites. Here, we used a random direct arylation polymerization (DARp) strategy in which the ratio of EDOT and Prodod can be tuned in the CPs; the large side chains can improve the solubility of the Prodod-EDOT copolymers. The oxidation potential of CPs reduces from P<sub>1</sub> to P<sub>3</sub> as the proportion of the electron rich unit EDOT increases (Figure S16). Therefore, P<sub>2</sub> and P<sub>3</sub> are most likely to be doped and form the most stable composite compared to P<sub>1</sub>. After doping, the P<sub>3</sub> composite observes the highest increase in conductivity. The conductivities of C<sub>M</sub>-Si/P<sub>1</sub>, C<sub>M</sub>-Si/P<sub>2</sub>, and C<sub>M</sub>-Si/P<sub>3</sub> increased by one order, five orders, and six orders of magnitude (Figure S17) from 10<sup>-6</sup> S/cm of their pure polymers, respectively. In the thermal stability test, C<sub>M</sub>-Si/P<sub>2</sub> and C<sub>M</sub>-Si/P<sub>3</sub> show better thermal stability than C<sub>M</sub>-Si/P<sub>1</sub>. After being baked at 353 K for 24 h, C<sub>M</sub>-Si/P<sub>2</sub> and C<sub>M</sub>-Si/P<sub>3</sub> maintained nearly 80% of their original conductivity while C<sub>M</sub>-Si/P<sub>1</sub> lost over 90% (Figure 5a, Figure S18). Additionally, C<sub>M</sub>-Si/P<sub>2</sub> and C<sub>M</sub>-Si/P<sub>3</sub> show much higher polaronic absorption and a smaller drop of bipolaronic absorption compared to C<sub>M</sub>-Si/P<sub>1</sub> under high temperature (Figure 5b–d).

### 3. CONCLUSION

In conclusion, we demonstrated the thermally stable and solvent-resistant conductive polymer composite by simply mixing cross-linkable chlorosilanes with dioxythiophene polymers. By introducing cross-linkable chlorosilanes, doping and the cross-link process occur simultaneously with the electrical conductivity of the composites increasing by up to six orders of magnitude compared with pure polymers. The presence of cross-linked siloxane network stabilizes the morphology of C-Si/CPs, which can effectively prevent the dedoping process at high temperature. With the most rigid cross-linked siloxane network, the C<sub>M</sub>-Si/P<sub>3</sub> composites exhibit the highest thermal stability, showing high polaronic absorption at 453 K and maintaining nearly 80% of the original conductivities after 24 h at 353 K in ambient conditions. Also, C-Si/CPs composites show promising solvent robustness. The results show that the combination of dopant

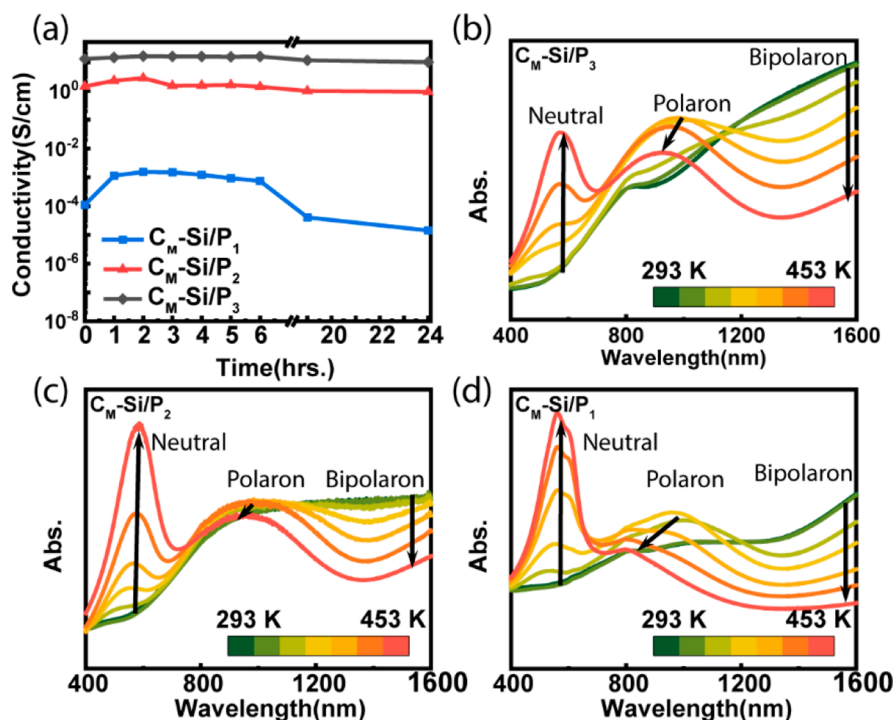


**Figure 5.** (a) Conductivities of 56 wt % C<sub>M</sub>-Si/CPs composites with different CPs when baked at 353 K under ambient conditions after 24 h; *in situ* temperature-dependent UV–vis absorption comparison with varying chlorosilanes (b) 56 wt % C<sub>M</sub>-Si/P<sub>1</sub>, (c) 56 wt % C<sub>M</sub>-Si/P<sub>2</sub>, and (d) 56 wt % C<sub>M</sub>-Si/P<sub>1</sub> when increasing temperature from 293 to 453 K.

and rigid cross-linked network could stabilize the film morphology and thus improve doping stability at harsh conditions.

#### 4. EXPERIMENTAL SECTION

**Materials.** All the chlorosilanes precursors, 1,6-bis(trichlorosilyl)hexane (Crosslinable Silane; C<sub>6</sub>-Si), 1,6-bis(chlorodimethylsilyl)hexane (Linear Silane; L<sub>6</sub>-Si), chlorotriethylsilane (Flowable Silane; F-Si), hexytrichlorosilane (C<sub>M</sub>-Si), and 1,10-bis(trichlorosilyl)dacane (C<sub>10</sub>-Si) are purchased from Gelest and used as received. P<sub>1</sub>, P<sub>2</sub>, and P<sub>3</sub> are synthesized and the details of the polymer synthesis can be found in [Supporting Information](#). All of the solvents used in the experiments were purchased from Sigma and used as received.

**Sample Preparation and Characterization.** All of the processing, doping, and characterization of composites are performed in ambient conditions. CPs are dissolved in chloroform with a concentration of 25 mg/L at 40 °C, and the chlorosilane solutions are prepared in chloroform with concentrations of 320, 160, 80, and 40 mg/mL. Chlorosilane solutions (200 μL) are added into 1 mL of CP solutions and the mixed solutions can be stored for 1–2 days before film processing. After 2 days, the solution will become too viscous, making it much harder to be used. Chlorosilanes/CP composites are deposited on the prepatterned substrate by spin-coating with a speed of 1500 rpm for 60 s with the thickness dependent on the content of chlorosilanes. All of the substrates are successively rinsed with DI water, soap, ethanol, acetone, and chloroform and dried by nitrogen before processing. After spin coating, the composites are dried in the oven for 10 min at 60 °C to enhance the formation of siloxane matrices and remove residual solvent.

**Morphology Analysis.** The thickness of films, height, and phase images are obtained using Cypher Asylum AFM and processed through Gwyddion Software.

**Electrical Conductivity Measurement.** The electrical conductivity was measured with two-probe and four-probe methods by Keithley 4200 under ambient environment. The conductivities obtained from two-probe method are similar to those measured by four-probe method, and the trend is overall the same. Films for two-

probe measurements were measured based on the bottom contact OFET configuration by applying a bias from –1 V to 1 V. Channel width (*W*) and length (*L*) used for all the two-probe measurements were 1000 and 100 μm, respectively. Four-probe method was also utilized to compare thermal stability of different samples during long-term baking tests. In the four-probe measurements, four gold contacts (with the inner two electrodes of *W/L* = 4) were deposited on the clean SiO<sub>2</sub> substrates through a prepatterned shadow mask at a rate of 0.8 Å/s to a final thickness of 30 nm. Films were processed as described in [Sample Preparation and Characterization](#).

***In Situ* Temperature-Dependent Measurements.** To control the thermal conditions both for electrical conductivity and UV–vis absorption measurements, the HFS600E-PB4 Linkam stage was used with the heating and cooling rates maintained at 10 °C/min. The devices were allowed to reach thermal equilibrium.

#### ■ ASSOCIATED CONTENT

##### Supporting Information

The Supporting Information is available free of charge at <https://pubs.acs.org/doi/10.1021/acsapm.0c01378>.

Synthetic route of CPs, AFM figures of different chlorosilanes/CPs composites, IR spectrum, CV of pure CPs ([PDF](#))

#### ■ AUTHOR INFORMATION

##### Corresponding Author

Jianguo Mei – Purdue University, West Lafayette, Indiana 47907, United States; [orcid.org/0000-0002-5743-2715](https://orcid.org/0000-0002-5743-2715); Email: [jgmei@purdue.edu](mailto:jgmei@purdue.edu)

##### Authors

Zhifan Ke – Purdue University, West Lafayette, Indiana 47907, United States  
Liyan You – Purdue University, West Lafayette, Indiana 47907, United States

Dung T. Tran – Purdue University, West Lafayette, Indiana 47907, United States

Jiazhi He – Purdue University, West Lafayette, Indiana 47907, United States

Kuluni Perera – Purdue University, West Lafayette, Indiana 47907, United States

Aristide Gumyusenge – Purdue University, West Lafayette, Indiana 47907, United States

Complete contact information is available at:  
<https://pubs.acs.org/10.1021/acsapm.0c01378>

### Author Contributions

All authors have given approval to the final version of the manuscript.

### Funding

This work was financially supported by Ambilight Inc.

### Notes

The authors declare the following competing financial interest(s): J.M. is a co-founder of Ambilight, which supports this study financially.

## REFERENCES

- (1) Lussem, B.; Keum, C. M.; Kasemann, D.; Naab, B.; Bao, Z.; Leo, K. Doped Organic Transistors. *Chem. Rev.* **2016**, *116* (22), 13714–13751.
- (2) Lüssem, B.; Riede, M.; Leo, K. Doping of organic semiconductors. *Phys. Status Solidi A* **2013**, *210* (1), 9–43.
- (3) Ponder, J. F.; Menon, A. K.; Dasari, R. R.; Pittelli, S. L.; Thorley, K. J.; Yee, S. K.; Marder, S. R.; Reynolds, J. R. Conductive, Solution-Processed Dioxathiophene Copolymers for Thermoelectric and Transparent Electrode Applications. *Adv. Energy Mater.* **2019**, *9*, 1900395.
- (4) Bubnova, O.; Khan, Z. U.; Malti, A.; Braun, S.; Fahlman, M.; Berggren, M.; Crispin, X. Optimization of the thermoelectric figure of merit in the conducting polymer poly (3, 4-ethylenedioxythiophene). *Nat. Mater.* **2011**, *10* (6), 429–433.
- (5) Kim, G.-H.; Shao, L.; Zhang, K.; Pipe, K. P. Engineered doping of organic semiconductors for enhanced thermoelectric efficiency. *Nat. Mater.* **2013**, *12* (8), 719–723.
- (6) Russ, B.; Gludell, A.; Urban, J. J.; Chabiny, M. L.; Segalman, R. A. Organic thermoelectric materials for energy harvesting and temperature control. *Nature Reviews Materials* **2016**, *1* (10), 1–14.
- (7) Xia, Y.; Sun, K.; Ouyang, J. Solution-processed metallic conducting polymer films as transparent electrode of optoelectronic devices. *Adv. Mater.* **2012**, *24* (18), 2436–2440.
- (8) Yang, Y.; Heeger, A. Polyaniline as a transparent electrode for polymer light-emitting diodes: Lower operating voltage and higher efficiency. *Appl. Phys. Lett.* **1994**, *64* (10), 1245–1247.
- (9) Root, S. E.; Alkhadra, M. A.; Rodriguez, D.; Printz, A. D.; Lipomi, D. J. Measuring the Glass Transition Temperature of Conjugated Polymer Films with Ultraviolet-Visible Spectroscopy. *Chem. Mater.* **2017**, *29* (7), 2646–2654.
- (10) Koizumi, H.; Dougauchi, H.; Ichikawa, T. Mechanism of dedoping processes of conducting poly (3-alkylthiophenes). *J. Phys. Chem. B* **2005**, *109* (32), 15288–15290.
- (11) Matveeva, E.; Calleja, R. D.; Sanchez-Martinez, E. AC conductivity of thermally dedoped polyaniline. *Synth. Met.* **1994**, *67* (1–3), 207–210.
- (12) Wang, Y.; Rubner, M. F. Electrically conductive semi-interpenetrating polymer networks of poly (3-octylthiophene). *Macromolecules* **1992**, *25* (12), 3284–3290.
- (13) Szabo, L.; Čík, G.; Lesný, J. Thermal stability increase of doped poly (3-hexadecylthiophene) by  $\gamma$ -radiation. *Synth. Met.* **1996**, *78* (2), 149–153.
- (14) Yim, K.-H.; Whiting, G. L.; Murphy, C. E.; Halls, J. J. M.; Burroughes, J. H.; Friend, R. H.; Kim, J.-S. Controlling Electrical Properties of Conjugated Polymers via a Solution-Based p-Type Doping. *Adv. Mater.* **2008**, *20* (17), 3319–3324.
- (15) Karpov, Y.; Erdmann, T.; Raguzin, I.; Al-Hussein, M.; Binner, M.; Lappan, U.; Stamm, M.; Gerasimov, K. L.; Beryozkina, T.; Bakulev, V.; Anokhin, D. V.; Ivanov, D. A.; Gunther, F.; Gemming, S.; Seifert, G.; Voit, B.; Di Pietro, R.; Kiriy, A. High Conductivity in Molecularly p-Doped Diketopyrrolopyrrole-Based Polymer: The Impact of a High Dopant Strength and Good Structural Order. *Adv. Mater.* **2016**, *28* (28), 6003–10.
- (16) Li, J.; Rochester, C. W.; Jacobs, I. E.; Friedrich, S.; Stroeve, P.; Riede, M.; Moule, A. J. Measurement of Small Molecular Dopant F4TCNQ and C60F36 Diffusion in Organic Bilayer Architectures. *ACS Appl. Mater. Interfaces* **2015**, *7* (51), 28420–8.
- (17) Li, J.; Koshnick, C.; Diallo, S. O.; Ackling, S.; Huang, D. M.; Jacobs, I. E.; Harrelson, T. F.; Hong, K.; Zhang, G.; Beckett, J.; Mascal, M.; Moulé, A. J. Quantitative Measurements of the Temperature-Dependent Microscopic and Macroscopic Dynamics of a Molecular Dopant in a Conjugated Polymer. *Macromolecules* **2017**, *50* (14), 5476–5489.
- (18) Gao, Z. Q.; Mi, B. X.; Xu, G. Z.; Wan, Y. Q.; Gong, M. L.; Cheah, K. W.; Chen, C. H. An organic p-type dopant with high thermal stability for an organic semiconductor. *Chem. Commun. (Cambridge, U. K.)* **2008**, No. 1, 117–9.
- (19) Vitoratos, E.; Sakkopoulos, S.; Dalas, E.; Paliatsas, N.; Karageorgopoulos, D.; Petraki, F.; Kennou, S.; Choulis, S. Thermal degradation mechanisms of PEDOT:PSS. *Org. Electron.* **2009**, *10* (1), 61–66.
- (20) Gumyusenge, A.; Tran, D. T.; Luo, X.; Pitch, G. M.; Zhao, Y.; Jenkins, K. A.; Dunn, T. J.; Ayzner, A. L.; Savoie, B. M.; Mei, J. Semiconducting polymer blends that exhibit stable charge transport at high temperatures. *Science* **2018**, *362* (6419), 1131–1134.
- (21) Gumyusenge, A.; Luo, X.; Ke, Z.; Tran, D. T.; Mei, J. Polyimide-Based High-Temperature Plastic Electronics. *ACS Materials Letters* **2019**, *1* (1), 154–157.
- (22) Khodagholy, D.; Doublet, T.; Quilichini, P.; Gurfinkel, M.; Leleux, P.; Ghestem, A.; Ismailova, E.; Herve, T.; Sanaur, S.; Bernard, C.; Malliaras, G. G. In vivo recordings of brain activity using organic transistors. *Nat. Commun.* **2013**, *4* (1), 1–7.
- (23) Rivnaya, J.; Inal, S.; Collins, B. A.; Sessolo, M.; Stavrinidou, E.; Strakosas, X.; Tassone, C.; Delongchamp, D. M.; Malliaras, G. G. Structural control of mixed ionic and electronic transport in conducting polymers. *Nat. Commun.* **2016**, *7* (1), 11287.
- (24) Zhang, S.; Kumar, P.; Nouas, A. S.; Fontaine, L.; Tang, H.; Cicoira, F. Solvent-induced changes in PEDOT: PSS films for organic electrochemical transistors. *APL Mater.* **2015**, *3* (1), 014911.
- (25) Park, H. W.; Choi, K. Y.; Shin, J.; Kang, B.; Hwang, H.; Choi, S.; Song, A.; Kim, J.; Kweon, H.; Kim, S.; Chung, K. B.; Kim, B.; Cho, K.; Kwon, S. K.; Kim, Y. H.; Kang, M. S.; Lee, H.; Kim, D. H. Universal Route to Impart Orthogonality to Polymer Semiconductors for Sub-Micrometer Tandem Electronics. *Adv. Mater.* **2019**, *31*, No. 1901400.
- (26) Shin, J.; Park, H. W.; Kim, S.; Yang, J.; Kim, J.; Park, H. W.; Kim, D. H.; Kang, M. S. Electrical transport characteristics of chemically robust PDPP-DTT embedded in a bridged silsesquioxane network. *J. Mater. Chem. C* **2019**, *7* (47), 14889–14896.
- (27) Yoon, M.-H.; Yan, H.; Facchetti, A.; Marks, T. J. Low-voltage organic field-effect transistors and inverters enabled by ultrathin cross-linked polymers as gate dielectrics. *J. Am. Chem. Soc.* **2005**, *127* (29), 10388–10395.
- (28) Kao, C. Y.; Lee, B.; Wielunski, L. S.; Heeney, M.; McCulloch, I.; Garfunkel, E.; Feldman, L. C.; Podzorov, V. Doping of Conjugated Polythiophenes with Alkyl Silanes. *Adv. Funct. Mater.* **2009**, *19* (12), 1906–1911.
- (29) Jeong, S.; Kim, D.; Park, B. K.; Lee, S.; Moon, J. Influence of silanol groups on the electrical performance of organic thin-film transistors utilizing organosiloxane-based organic-inorganic hybrid dielectrics. *Nanotechnology* **2007**, *18* (2), 025204.
- (30) Kim, C.; Wang, Z.; Choi, H.-J.; Ha, Y.-G.; Facchetti, A.; Marks, T. J. Printable cross-linked polymer blend dielectrics. Design

strategies, synthesis, microstructures, and electrical properties, with organic field-effect transistors as testbeds. *J. Am. Chem. Soc.* **2008**, *130* (21), 6867–6878.

(31) Choi, S.-S.; Lee, A. S.; Lee, H. S.; Jeon, H. Y.; Baek, K.-Y.; Choi, D. H.; Hwang, S. S. Synthesis and characterization of UV-curable ladder-like polysilsesquioxane. *J. Polym. Sci., Part A: Polym. Chem.* **2011**, *49* (23), 5012–5018.

(32) Seki, H.; Kajiwara, T.; Abe, Y.; Gunji, T. Synthesis and structure of ladder polymethylsilsesquioxanes from sila-functionalized cyclotetrasiloxanes. *J. Organomet. Chem.* **2010**, *695* (9), 1363–1369.

(33) Loy, D. A.; Shea, K. J. Bridged polysilsesquioxanes. Highly porous hybrid organic-inorganic materials. *Chem. Rev.* **1995**, *95* (5), 1431–1442.

(34) Oviatt, H. W., Jr; Shea, K. J.; Small, J. H. Alkylene-bridged silsesquioxane sol-gel synthesis and xerogel characterization. Molecular requirements for porosity. *Chem. Mater.* **1993**, *5* (7), 943–950.